GIPR Agonism Inhibits PYY-Induced Nausea-Like Behavior

Ricardo J. Samms,[1] Richard Cosgrove,[1] Brandy M. Snider,[1] Ellen C. Furber,[1] Brian A. Droz,[1] Daniel A. Briere,[1] James Dunbar,[1] Mridula Dogra,[1] Jorge Alsina-Fernandez,[1] Tito Borner,[2,3] Bart C. De Jonghe,[2,3] Matthew R. Hayes,[2,3] Tamer Coskun,[1] Kyle W. Sloop,[1] Paul J. Emmerson,[1] and Minrong Ai[1]

Diabetes 2022;71:1410–1423 | https://doi.org/10.2337/db21-0848

The induction of nausea and emesis is a major barrier to maximizing the weight loss profile of obesity medications, and therefore, identifying mechanisms that improve tolerability could result in added therapeutic benefit. The development of peptide YY (PYY)-based approaches to treat obesity are no exception, as PYY receptor agonism is often accompanied by nausea and vomiting. Here, we sought to determine whether glucose-dependent insulinotropic polypeptide (GIP) receptor (GIPR) agonism reduces PYY-induced nausea-like behavior in mice. We found that central and peripheral administration of a GIPR agonist reduced conditioned taste avoidance (CTA) without affecting hypophagia mediated by a PYY analog. The receptors for GIP and PYY (*Gipr* and *Npy2r*) were found to be expressed by the same neurons in the area postrema (AP), a brainstem nucleus involved in detecting aversive stimuli. Peripheral administration of a GIPR agonist induced neuronal activation (cFos) in the AP. Further, whole-brain cFos analyses indicated that PYY-induced CTA was associated with augmented neuronal activity in the parabrachial nucleus (PBN), a brainstem nucleus that relays aversive/emetic signals to brain regions that control feeding behavior. Importantly, GIPR agonism reduced PYY-mediated neuronal activity in the PBN, providing a potential mechanistic explanation for how GIPR agonist treatment reduces PYY-induced nausea-like behavior. Together, the results of our study indicate a novel mechanism by which GIP-based therapeutics may have benefit in improving the tolerability of weight loss agents.

A major challenge of current and novel weight loss medications is the occurrence of nausea and vomiting (1–3). These physiological responses can occur due to drug-mediated overstimulation of anorectic pathways and/or the recruitment of aversive/emetic circuits that naturally defend against the consumption of toxic substances (4–6). Aversive/emetic responses are largely controlled by the area postrema (AP), a circumventricular organ located in the hindbrain that senses blood-borne signals (7). The AP plays a dual role in detecting both satiety and emetic signals (7–9). Therefore, identifying therapeutic agents that target nonaversive anorectic circuits originating within the AP offers great potential for the treatment of conditions exacerbated by excess energy consumption such as type 2 diabetes (T2D) and obesity.

Glucose-dependent insulinotropic polypeptide (GIP) is a gut-derived hormone that enhances glucose-dependent insulin secretion, thereby helping to regulate postprandial glycemia (10). In addition to its role as an incretin, GIP can act centrally to impact energy homeostasis (11). Indeed, the GIP receptor (GIPR) is expressed by both glutamatergic and GABAergic neurons found in hypothalamic nuclei that regulate energy balance (e.g., the arcuate [ARC], paraventricular [PVH], and dorsomedial [DMH] nuclei) and by GABAergic neurons in the AP (12–14). Peripheral administration of GIPR agonists induces neuronal activation in the ARC and AP (14,15). Additionally, chemogenetic activation of $GIPR^{+}$ cells in the ARC reduces feeding in mice (12),

[1]Lilly Research Laboratories, Lilly Corporate Center, Indianapolis, IN
[2]Department of Psychiatry, Perelman School of Medicine, University of Pennsylvania, Philadelphia, PA
[3]Department of Biobehavioral Health Sciences, School of Nursing, University of Pennsylvania, Philadelphia, PA

Corresponding authors: Ricardo J. Samms, samms_ricardo_j@lilly.com, and Minrong Ai, ai_minrong@lilly.com

Received 23 September 2021 and accepted 29 March 2022

This article contains supplementary material online at https://doi.org/10.2337/figshare.19601518.

and both central and peripheral administration of GIPR agonists reduces food intake and body weight in obese mice (15,16). Further, chronic treatment of obese mice with GIPR agonists enhances the anorectic action of glucagon-like peptide 1 receptor (GLP-1R) agonism and delivers synergistic weight loss (17). Intriguingly, in addition to enhancing the anorectic action of GLP-1R agonism, GIPR activation has been shown to block emesis in ferrets, musk shrews, and dogs and attenuate nausea-like behavior in mice and rats (14,18,19). This work has led to the hypothesis that GIPR agonism enhances the weight loss efficacy of GLP-1R agonism, in part, by attenuating its nauseating activity and thereby improving patient compliance (20–22). If true, these findings have significant implications not only for the GLP-1R agonist drug class but also for other anorectic agents whose weight loss efficacy is compromised by tolerability issues.

One obesity drug candidate whose anorectic activity may be linked to inducing a state of visceral malaise is peptide tyrosine-tyrosine (PYY_{3-36}) (23,24). PYY_{3-36} is a gut-derived hormone that promotes satiety by activating the neuropeptide Y receptor type 2 (NPY2R) in the hypothalamus and brainstem (24,25). However, efforts to develop PYY-based approaches to treat obesity have been hampered by the occurrence of nausea and vomiting on treatment with PYY-derived analogs (26,27). Therefore, the objective of the current investigation was to determine whether treatment with a GIPR agonist blocks nausea-like behavior induced by a PYY analog. We took an integrated approach combining behavioral indices of nausea with whole-brain neuronal activity mapping. With these approaches we determined that GIPR agonism attenuates the aversive effect of a PYY analog while maintaining its anorectic activity. Mechanistically, we show that the GIPR and NPY2R are expressed by the same neurons in the AP, and we describe a neural pathway by which GIPR agonism may mitigate malaise induced by a PYY analog.

RESEARCH DESIGN AND METHODS

Peptide Synthesis and In Vitro Characterization

GIPR agonists (short acting [GIPRA] and long acting [LAGIPRA] [19]), and a NPY2 selective long-acting analog of PYY (compound 4 [28]), were synthesized at Eli Lilly and Company. cAMP assays were conducted in HEK293 cells expressing the mouse GLP-1R, GIPR, or GCGR or mouse NPY2R using a homogeneous time-resolved fluorescence method to assess cAMP accumulation or the inhibition of forskolin-mediated stimulation of cAMP (CisBio cAMP Dynamic 2 HTRF assay kit, 62AM4PEJ). We determined intracellular cAMP levels by extrapolation using a standard curve. Dose response curves of compounds were plotted as the percentage of stimulation normalized to minimum and maximum values and analyzed with a four-parameter nonlinear regression fit with a variable slope (Genedata Screener 13).

Animals

All experiments were performed in accordance with protocols approved by the Eli Lilly and Co. Institutional Animal Care and Use Committee. All animals were individually housed in a temperature-controlled facility with a 12 h/12 h light/dark cycle. Wild-type (WT) and *Gipr*-deficient ($Gipr^{-/-}$) mice on a C57BL/6 genetic background (29,30) were maintained at Taconic Contract Breeding.

Pharmacokinetic Analysis

The pharmacokinetic (PK) of LAGIPRA and a long-acting PYY (LAPYY) analog was evaluated in male CD-1 mice following a single dose of 200 nmol/kg s.c. Blood samples were collected over 168 h, and the resulting individual concentrations from one or two animals/group/time point were used to calculate the reported PK parameters. The PK parameters are shown in Supplementary Table 1.

Conditioned Taste Avoidance Assay

Conditioned taste avoidance (CTA) was established as previously described (31). Age-matched (10–12 weeks) male WT mice (C57BL/6) were individually housed with ad libitum access to food and water. Two water bottles were placed into each cage with equal access to food on both sides. Day −1, water bottles were removed and overnight (18 h) water deprivation was initiated to facilitate drinking on day 1. On day 1, mice were given access to two bottles, each filled with a saccharin solution (0.15%), for 40 min and immediately thereafter given an injection of each respective aversive agent (PYY [via subcutaneous injection], LiCl [via interparental injection] [cat. no. 501821911; Sigma-Aldrich], or recombinant human GDF15 [via interparental injection] alone or in combination with vehicle, GIPRA [subcutaneously], or LAGIPRA [subcutaneously]; n = 6 per group). Following compound administration bottles were removed, and bottles containing just water were returned. On day 4, mice were water deprived overnight (∼18 h). On day 5, mice were given one bottle containing water and one bottle containing the saccharin solution (0.15%), and placement of bottles was counterbalanced across all animals to prevent a conditioned place preference effect. On day 6, 24 h after the two-bottle choice test, each bottle was removed and weighed and the saccharin preference ratio was calculated. Twenty-four-hour body weight and food intake were recorded.

Intracerebroventricular Cannulation

Mice were intracerebroventricularly cannulated by insertion of a unilateral site-directed guide cannula (mouse cannula, 2 mm, PlasticsOne, Bilaney, Germany) into the right lateral ventricle under isoflurane anesthesia (Vetflurane; Virbac, Kolding, Denmark). An incision was made along the midline of the skull, and two holes (one rostral in the right frontal bone and one caudal in the left parietal bone) were drilled, followed by insertion of anchoring screws. A cannula hole was drilled and the cannula placed and fastened with use of acrylic dental

cement at the following coordinates: anterior-posterior −0.25, medial-lateral 1.0, and caudal-ventral −2 mm relative to bregma. Carprofen (Norodyl; ScanVet, Fredensborg, Denmark) and enrofloxacin (Baytril; Bayer, Leverkusen, Germany) were administered on the day of operation and for the following 3 days.

cFos Analysis

For all cFos studies, chow-fed C57BL/6J male mice were acclimated to handling with daily PBS injection (subcutaneously) for 4 days. On day 5, GIPRA (10 nmol/kg s.c.), PYY (100 nmol/kg s.c.), and GDF15 (2 nmol/kg s.c.) and combinations thereof were dosed. Mice were anesthetized and transcardially perfused with 10% formalin at 45 min (Fig. 6 and Supplementary Fig. 4) or 120 min (Figs. 7 and 8 and Supplementary Figs. 5 and 6) post–drug injection. Brain samples were collected, prepared, and cleared according to standard iDISCO+ protocol. cFos immunostaining, light sheet microscopy, image processing, registration and voxel-based statistical analysis were performed exactly as previously described (32). The three-dimensional cFos hotspots at parabrachial nucleus (PBN) (dorsal PBN [PBN_D] and ventral PBN [PBN_V]) were defined by the averaged cFos signal in PYY-treated group and GDF15–treated group, respectively. Subsequent cFos quantification with voxel-based statistical analysis was performed within these registered three-dimensional hotspots for each treatment group. Immunohistochemistry antibodies were as follows: rabbit anti-cFos (1:200, 9F6; Cell Signaling Technology), sheep anti-FoxP2 (1:5,000, AF5647; R&D Systems), guinea pig anti-CGRP (1:500, no. 14004; Synaptic Systems), and sheep anti-GFRAL (1:1,000, AF5728; R&D Systems).

RNAscope In Situ Hybridization

In situ hybridization studies were conducted with use of the RNAscope method (Advanced Cell Diagnostics, Newark, CA). Mice (C57BL6J; Janvier Labs) or rats (Long Evans; Janvier Labs) were terminally anesthetized and the brains removed and frozen on dry ice. Brains were sectioned (coronal sections covering the AP and nucleus tractus solitaries [NTS]) on a cryostat (12 μm) and mounted on microscope slides. Cynomolgus monkey brain block containing the AP was obtained from MediTox (Czech Republic) and fixed in 10% neutral buffered formalin for 24 h before transfer to 70% ethanol followed by paraffin imbedding and sectioning (5 μm). Sections were stained with RNAscope multiplex probes (mouse, Gipr 319121-C2, Npy1r 427021-C1, Npy2r 315951-C1, Npy4r 313551-C1, Npy5r custom designed by Advanced Cell Diagnostics; rat, Gipr 318801-C2, Npy1r 414471-C1, Npy2r 414481-C1, Npy4r 414491-C1, Npy5r 414501-C1; and monkey, GIPR 49051-C2, NPY2R 508001-C1) according to the manufacturer's instructions. Sections were counterstained with DAPI to mark cellular nuclei, cover slipped, imaged, and scanned with an Olympus VS120 fluorescent scanner. Target mRNA and colocalization were then evaluated and reported. All experiments were conducted at Gubra (Hørsholm, Denmark).

Statistical Analysis

Data are presented as means ± SEM. Data analysis was conducted with GraphPad Prism 9. Statistical analyses performed included Student unpaired *t* test or one-way ANOVA or two-way ANOVA followed by Dunnett multiple comparisons test where appropriate. Differences were considered significant when $P < 0.05$.

Data and Resource Availability

The data sets generated during or analyzed during the current study are available from the corresponding author on reasonable request.

RESULTS

GIPR Agonism Enhances the Anorexic Action of PYY

To determine whether combined treatment of a GIPR agonist and PYY analog achieves a greater reduction in body weight and food intake in obese high-fat-fed mice, we used a potent and selective LAGIPRA (Supplementary Fig. 1*A* and Supplementary Table 1) (19) and an LAPYY analog with potent activity at the mouse Npy2 receptor (Supplementary Fig. 1*B* and Supplementary Table 1) (28). Following a single dose (200 nmol/kg s.c.) of LAGIPRA or the LAPYY analog, the mean apparent clearance and mean half-life were 4.86 mL/h/kg and 21.3 h and 4.52 mL/h/kg and 20.7 h, respectively, in mice. (See Supplementary Table 2.) In vivo, LAGIPRA showed selectivity for the mouse GIPR by lowering blood glucose in intraperitoneal glucose tolerance tests in WT mice (Supplementary Fig. 2*A*) but not $Gipr^{-/-}$ mice (Supplementary Fig. 2*B*). In addition, the LAPYY analog dose-dependently decreased fasting-induced hyperphagia and weight gain in lean WT animals (Supplementary Fig. 2*C* and *D*). To determine whether GIPR agonism enhances the anorectic action of the LAPYY analog, we dosed obese mice chronically with the LAPYY analog alone or in combination with the LAGIPRA (Fig. 1). Both the LAPYY analog and LAGIPRA reduced food intake and body weight during a 72-h dosing period (Fig. 1*A*–*F*). Importantly, the LAGIPRA enhanced the anorectic action of low (3 nmol/kg) (Fig. 1*B*) and mid (30 nmol/kg) (Fig. 1*C*) doses of the LAPYY analog but only delivered greater weight loss in combination with a low dose of the LAPYY analog (Fig. 1*A*). These findings are the first to show that, similar to GLP-1R agonism, chronic treatment with an LAGIPRA enhances the anorectic and weight-lowering efficacy of a LAPYY analog in obese mice.

GIPR Agonism Attenuates PYY-Induced Aversion in Mice

To investigate the potential antiaversive action of GIPR agonism, we used both the LAGIPRA and a potent and selective GIPRA (19). (See Supplementary Fig. 1*C* and Supplementary Table 1.) In vivo, the GIPRA showed selectivity for the mouse GIPR by dose-dependently reducing

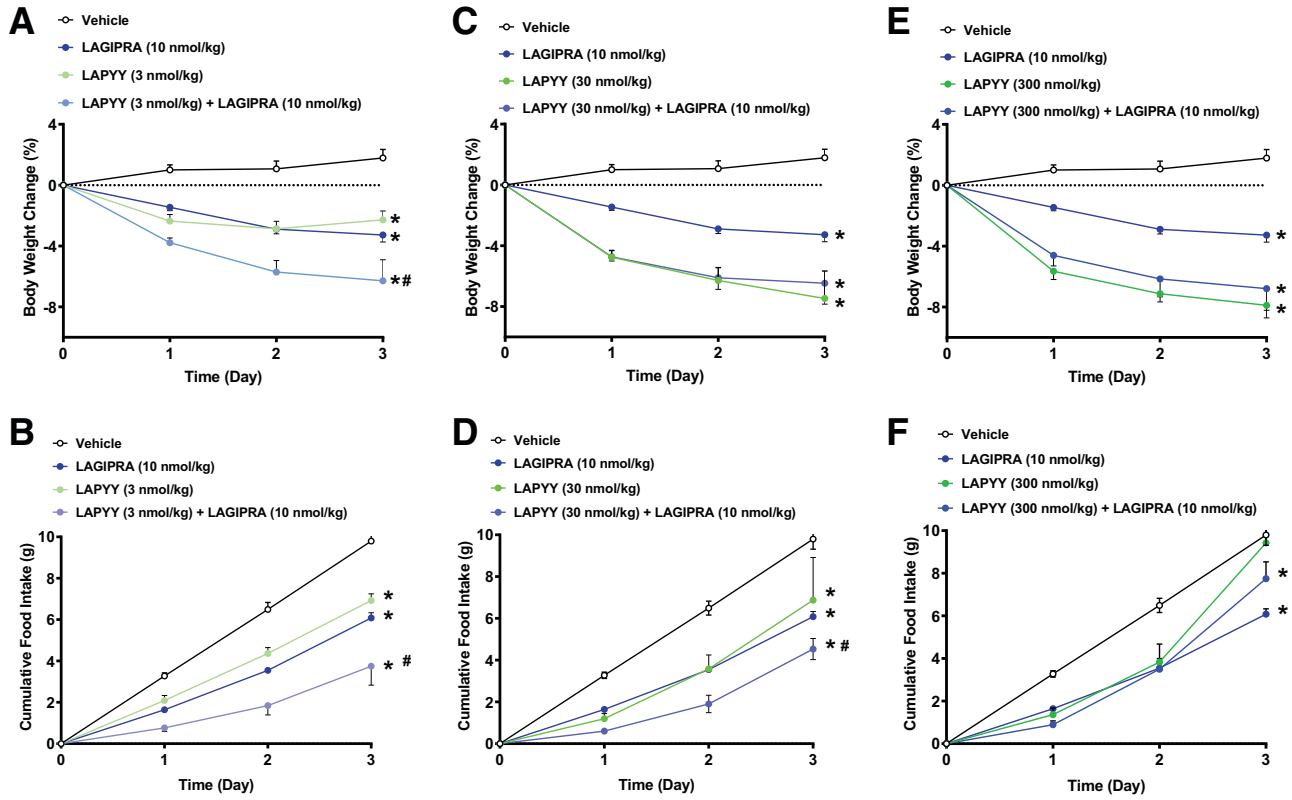

Figure 1—GIPR agonism enhances the anorectic action of PYY. Body weight and food intake in obese mice dosed once daily with an LAPYY analog at 3 nmol/kg (*A* and *B*), 10 nmol/kg (*C* and *D*), and 300 nmol/kg (*E* and *F*) alone or in combination with an LAGIPRA (10 nmol/kg) ($n = 6$ per group). Values are means ± SEM. *$P < 0.05$ vs. vehicle; #LAPYY vs. LAGIPRA + LAPYY.

hyperglycemia following an intraperitoneal glucose tolerance test in WT mice but not *Gipr*$^{-/-}$ mice (Supplementary Fig. 2*E* and *F*). To determine whether GIPR agonism attenuates the aversive effect of PYY, we applied the CTA assay, where exposure to a LAPYY analog was paired with a novel tastant (0.15% saccharin in drinking water) alone or in combination with either GIPRA or LAGIPRA. In this design, reduced consumption of the saccharin-containing solution is indicative of an aversive response. Consistent with previous reports (24), administration of the LAPYY analog dose-dependently reduced saccharin preference, food intake, and body weight in lean C57/B6 mice (Fig. 2*A*, *C*, and *E* and Supplementary Fig. 3*A*, *C*, and *E*). By contrast, there was no effect of either GIPRA (Fig. 2*A*) or LAGIPRA (Supplementary Fig. 3*B*) on saccharin preference compared with vehicle treatment. Strikingly, in the presence of either GIPR agonist, the aversive effect of the LAPYY analog was ablated at all effective doses tested (Fig. 2*B* and Supplementary Fig. 3*B*); of note, the LAPYY analog still reduced 24 h food intake and body weight (Fig. 2*D* and *F* and Supplementary Fig. 3*D* and *F*).

GIP has been shown to require its receptor in the central nervous system (CNS) to suppress appetite (15). Therefore, to determine whether the GIPRA can act centrally to block PYY-induced CTA, we administered the GIPRA via an intracerebroventricular injection, while the LAPYY analog was dosed peripherally. Consistent with data from GIPRA peripheral dosing (Fig. 3*A*, *C*, and *E*), central administration of the GIPRA ablated the aversive effect of the LAPYY analog (Fig. 3*B*) without affecting the ability of the LAPYY analog to suppress food intake and reduce body weight (Fig. 3*D* and *F*). The finding that GIPR agonism attenuates the aversive effect of PYY without altering its hypophagic effect provides new insight into the mechanisms whereby GIPR agonism may offer therapeutic advantages.

To determine whether the antiaversive action of GIPR agonism is specific to meal-related satiety factors (e.g., PYY) or extends to broad emetic stimuli, we investigated the effect of the GIPRA on CTA induced by the abdominal irritant LiCl and the cytokine GDF15 (33). LiCl robustly provoked an aversive response (Fig. 4*A*); however, the GIPRA was unable to block this effect (Fig. 4*B*). GDF15-induced gastrointestinal malaise is mediated through binding to its receptor (GFRAL) on neurons located in the AP and NTS (31,33). Importantly, the GIPR is expressed by a population of neurons different from those of GFRAL in the AP (13,18). Therefore, we determined whether the GIPRA was able to block the known effect of GDF15 on CTA. GDF15 dose-dependently reduced saccharine preference (Fig. 4*C*). However, the GIPRA did not block the aversive action of GDF15 (Fig. 4*D*). Taken together, these

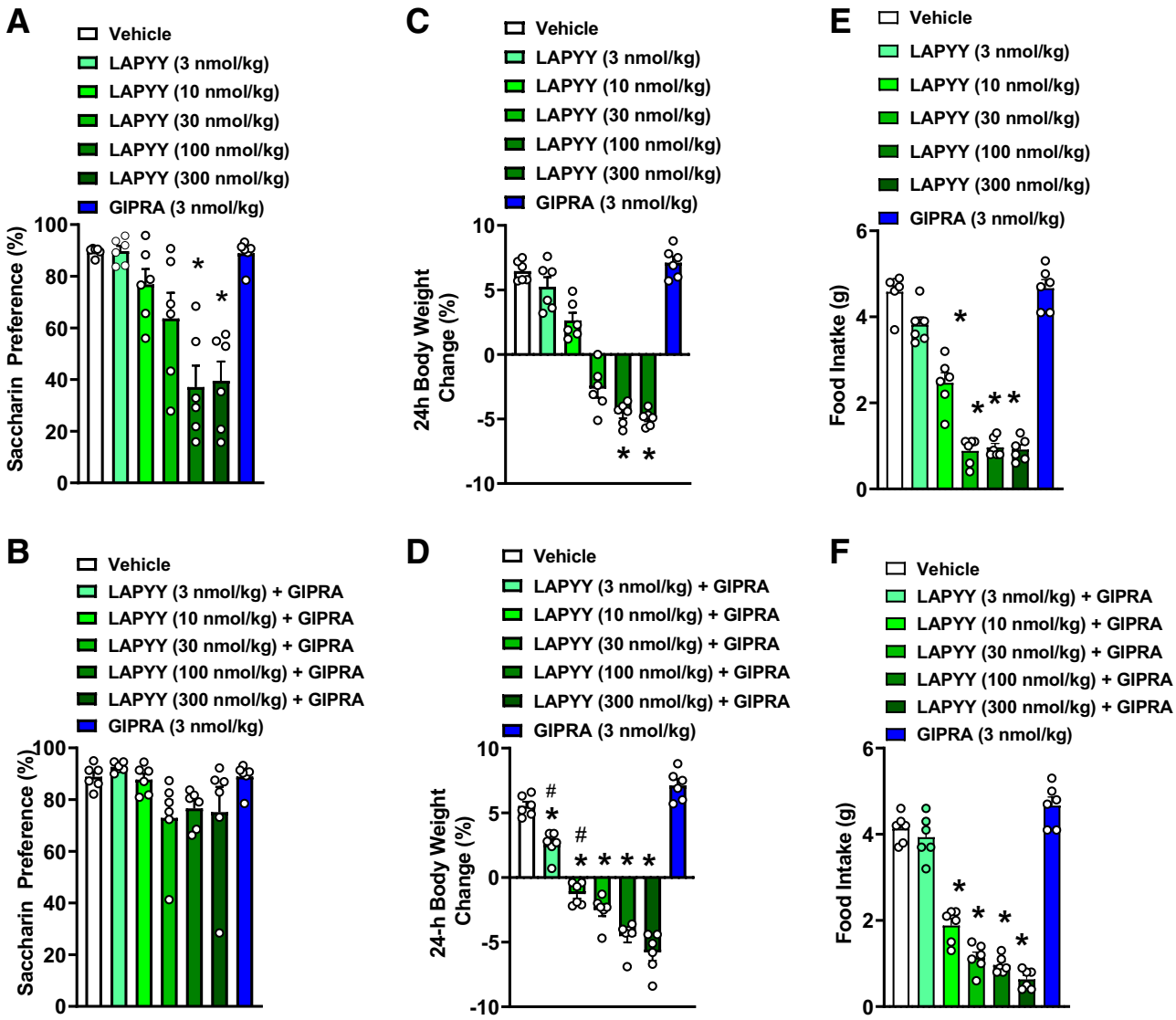

Figure 2—GIPR agonism attenuates PYY-induced aversion in mice. Saccharin preference (*A* and *B*) and 24 h body weight (*C* and *D*) and food intake (*E* and *F*) in lean C57/Bl6 mice dosed subcutaneously with an LAPYY analog alone (*A*, *C*, and *E*) or in combination (*B*, *D*, and *F*) with a GIPRA ($n = 6$ per group). Values are means ± SEM. *$P < 0.05$ vs vehicle; #$P < 0.05$ vs. LAPYY-only group. Statistical analyses performed with use of one-way ANOVA, followed by Dunnett multiple comparisons test where appropriate.

studies suggest that the antiaversive effect of GIP may be specific to meal-related factors that drive nausea-like behavior via neuronal circuits distinct from those of broad nauseating agents.

The GIPR and NPY2R Colocalize on Neurons in the AP in Mouse, Rat, and Monkey

To determine the expression pattern of *Gipr* and *Npy2r* in the AP and NTS, we conducted RNA insitu hybridization. In the mouse brain, cells expressing messages for the *Npy2r* were detected in the AP, as well as in scattered cells across the NTS. *Gipr* message was confined to cells in the AP, with few cells positive for *Gipr* in the neighboring NTS. Interestingly, in mice many *Gipr*-expressing cells were also found to express *Npy2r* (mean ± SEM 43 ± 4.6%) (Fig. 5*A* and *D*). While mRNA for other PYY receptors (Y1, Y4, and Y5) was detected in cells of the mouse AP, only limited colocalization with *Gipr* was observed (Fig. 5*D*). Of note, similar colocalization of *Gipr* and *Npy2r* (60.0 ± 2.4%) was detected in the rat brainstem (Fig. 5*B* and *D*). Consistent with the expression pattern in rodents, *Gipr* and *Npy2r* colocalized in cells of the monkey AP (Fig. 4*C* and *D*). Taken together, these data suggest a potential site of interaction whereby GIPR agonism may directly attenuate the ability of PYY to induce visceral malaise.

GIP Induces Neuronal Activity in the AP

Since the GIPR and NPY2R are coexpressed by a substantial number of neurons within the AP, we investigated

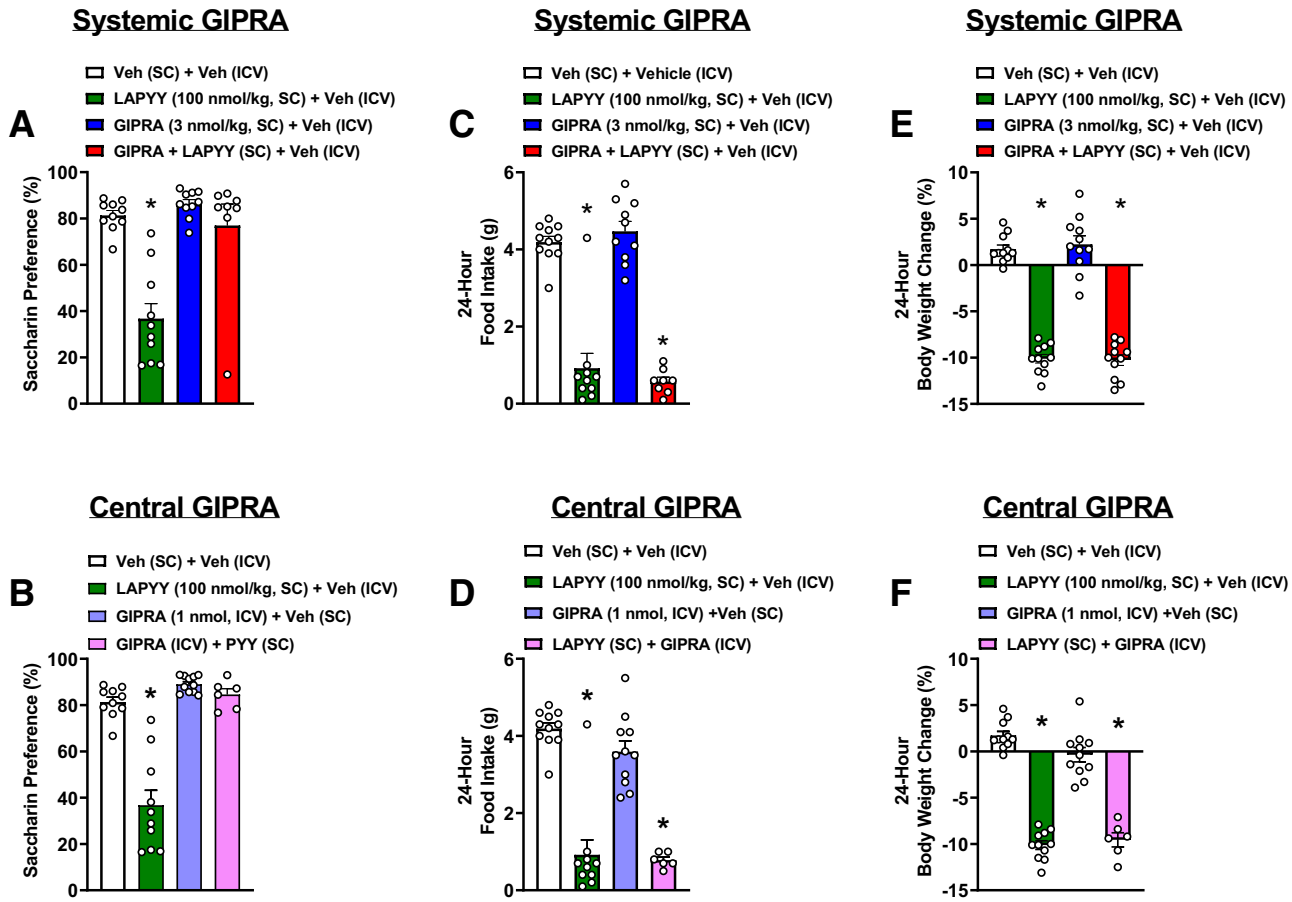

Figure 3—GIPR agonism attenuates PYY-induced aversion in mice. Saccharin preference (*A* and *B*) and food intake (*C* and *D*) and 24 h body weight (*E* and *F*) in lean C57/Bl6 mice dosed subcutaneously (SC) with an LAPYY agonist alone (*C* and *D*) and in combination (*E* and *F*) with a GIPRA dosed peripherally or centrally (intracerebroventricular injection [ICV]) (n = 6–11 per group). Values are means ± SEM. *$P < 0.05$ vs. vehicle (Veh). Statistical analyses performed included Student unpaired t test or one-way ANOVA, followed by Dunnett multiple comparisons test where appropriate.

whether peripherally dosed GIPRA and the LAPYY analog induce neuronal activity (cFos expression) in the AP and how GIPR and NPY2R agonism affects neuronal activity in this area of the brain. The GIPRA induced cFos expression in the mouse AP 45 min after injection (Fig. 6*A*, *B*, and *E*), while there was no cFos induced by LAPYY analog (Fig. 6*C* and *E*). Interestingly, cotreatment with the GIPRA and LAPYY analog led to a significant reduction of cFos expression compared with GIPRA treatment alone (Fig. 6*D* and *E*). We further conducted triple RNA in situ hybridization to detect cFos, Npy2r and Gipr in the AP and discovered that the GIPRA led to cFos expression in NPY2R$^+$ neurons, while the LAPYY analog and GIPRA cotreatment resulted in decreased cFos expression in these neurons (Supplementary Fig. 4). These results suggest that the activation of the G_i-coupled NPY2R does not induce cFos expression in NPY2R$^+$ AP neurons; however, it is capable of suppressing the cFos expression induced by the activation of G_s-coupled GIPR expressed in the same neurons (13). Further, in line with the differential effect of GIPRA treatment on PYY-induced CTA, compared with that of GDF15, we found that AP neurons activated by the GIPRA do not express GDF15 receptor GFRAL, suggesting that GIP and GDF15 engage distinct neuronal populations in the AP (Fig. 6*G* and *H*).

Next, we investigated how the GIPRA and LAPYY analog affect neuronal activity in the NTS. Interestingly, while neither the GIPRA nor LAPYY induced cFos expression when dosed alone (Fig. 6*F*), cotreatment with these agents robustly augmented cFos expression in the NTS (Fig. 6*F*). Overall, these results suggest that GIPRA and PYY directly impact the NPY2R$^+$ neurons in AP and engage neural pathways distinct from those recruited by GDF15.

Distinct cFos Expression Patterns Induced by GIPRA, PYY, and GDF15

Our invivo studies showed that GIP can block the aversive action of PYY but not that of the emetic agent GDF15. Therefore, to elucidate the downstream neuronal circuits

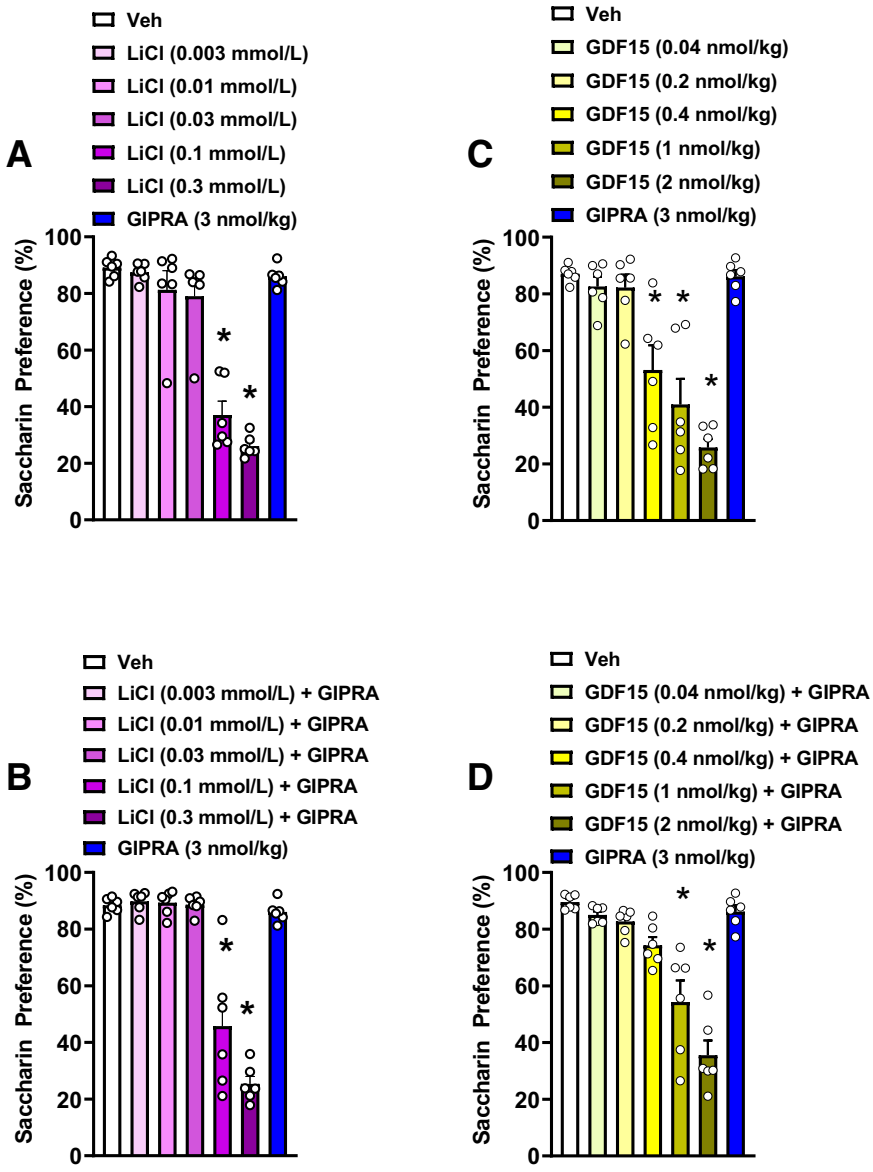

Figure 4—GIPR agonism does attenuate CTA induced by broad aversive agents. Saccharin preference ratio in lean C57/Bl6 mice dosed once with LiCl (intraperitoneally) and growth differentiation factor 15 (GDF15) (subcutaneously) alone (*A* and *C*) and in combination (*B* and *D*) with a GIPRA (subcutaneously) ($n = 6$ per group). Values are means ± SEM. *$P < 0.05$ vs. vehicle (Veh). Statistical analyses performed included a one-way ANOVA, followed by Dunnett multiple comparisons test where appropriate.

that may be responsible for the selective antiaversive action of GIPR agonism, we compared the effect of GIPRA on neuronal activity (cFos) induced by the LAPYY analog or GDF15 at 120 min posttreatments at the whole-brain level. Unbiased analysis showed that treatment with GIP increased cFos expression in four major regions of the CNS (i.e., the central amygdala [CeA], AP, xiphoid thalamus, and bed nuclei of the striata [BST]) (Fig. 7*A* and *F*). Treatment with the LAPYY analog augmented cFos expression in six regions of the brain (the CeA, PBN, AP, tuberal nucleus, retrochiasmatic area, and NTS) (Fig. 7*B* and *G*). Administration of GDF15 led to increased cFos expression in seven brain areas (the CeA, NTS, dorsal motor nucleus of the vagus [DMX], AP, paraventricular thalamus, BST, and PBN) and decreased cFos expression in nine regions (the gigantocellular reticular nucleus, posterolateral visual area, medial septum, VlSpl, tenia tecta dorsal part, posterior amygdala, nucleus accumbens core, reticular nucleus of the thalamus, and rostral linear nucleus raphe) (Fig. 7*C* and *H*).

The overall cFos expression patterns in animals receiving cotreatment of either the GIPRA and LAPYY analog or GIPRA and GDF15 were similar to those induced by the GIPRA or GDF15 treatments alone (Fig. 7*A*, *C–F*, and *H–J*). We quantified the number of $cFos^+$ cells in several brain regions that are known to be involved in the regulation of energy homeostasis, reward, or aversive behaviors,

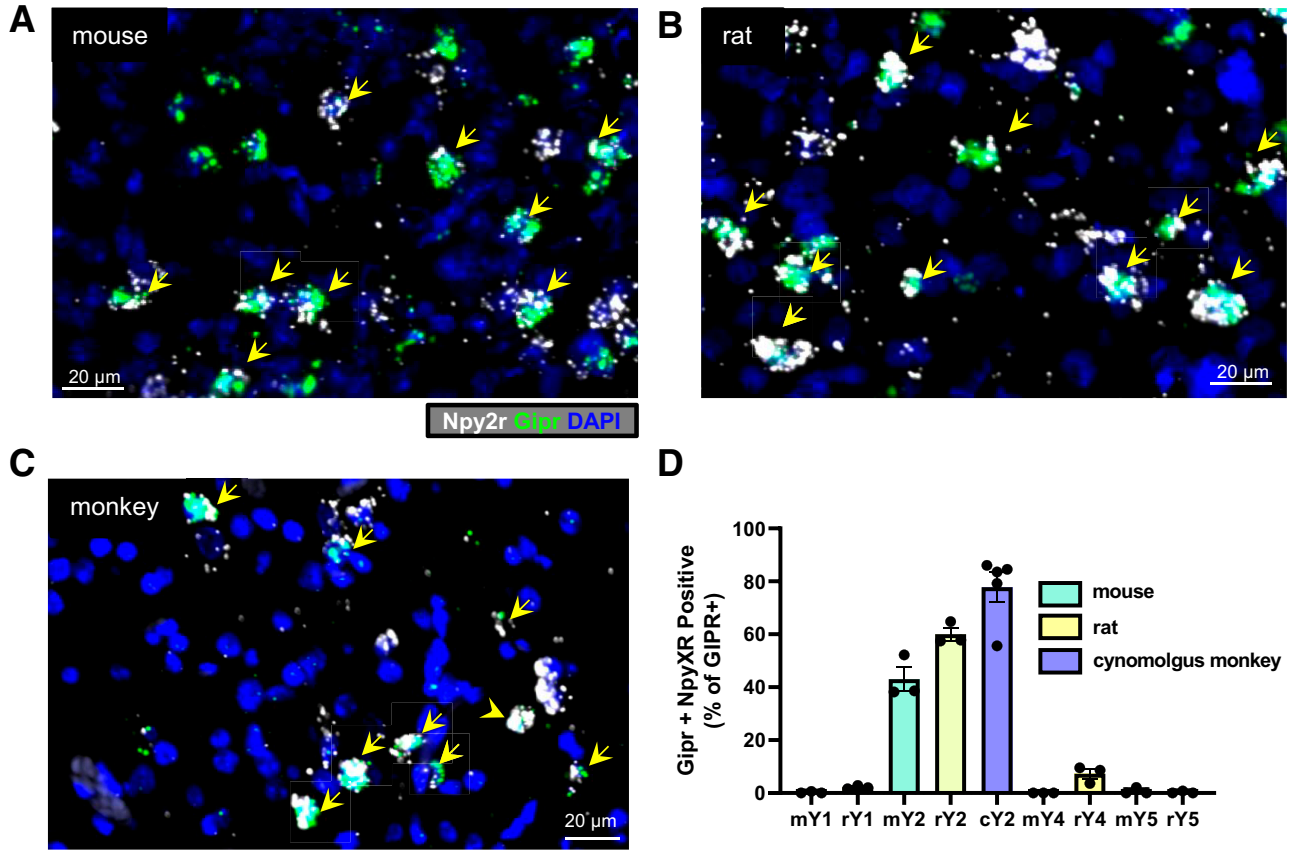

Figure 5—Specific colocalization of Gipr with Npy2R in mouse, rat, and monkey. Dual-label fluorescence in situ hybridization showing colocalization of Gipr (green) and Npy2r (white) mRNA transcripts in sections containing the AP from mouse (*A*), rat (*B*), and cynomolgus monkey (*C*). Nuclear staining (DAPI, blue) was used to identify brain regions. Yellow arrows indicate Gipr and Npy2r double-labeled cells. Colocalization of Gipr with Npy1, 2, 4, and 5 was assessed in sections from mouse and rat (n = 3) and Gipr with Npy2r in sections from cynomolgus monkey (5 sections from n = 2 monkeys). The percent colocalization (mean and SEM) of Gipr with mouse, rat or cynomolgus monkey NPY1R, NPY2R, NPY4R, and NPY5R (mY1, rY1, mY2, rY2, cY2, mY4, rY4, mY5, rY5).

including the AP, NTS, DMX, ARC, PVH, DMH, ventral medial hypothalamus, PBN, CeA, BST, nucleus accumbens, and ventral tegmental area. The number of cFos$^+$ cells were not statistically different in the ARC, DMH, Ventral medial hypothalamus, PVH, ACB, or ventral tegmental area among all treatment groups (Supplementary Fig. 5*B*–*G*). However, consistent with our finding in the AP at the 45 min time point (Fig. 6*E*), cotreatment with the GIPRA and LAPYY analog resulted in a moderately decreased expression of cFos at the 120 min time point compared with that of animals treated with the GIPRA alone (Fig. 7*K*). By contrast, cotreatment with the GIPRA and GDF15 led to a small increase of cFos expression in the AP compared with treatment with either GIPRA or GDF15 (Fig. 7*K*). In the neighboring nuclei of the NTS and DMX, treatment with GDF15 alone or in combination with GIPRA resulted in an increased number of cFos$^+$ cells (Fig. 7*L* and Supplementary Fig. 5*A*). In the CeA, cotreatment with the GIPRA and LAPYY or the GIPRA and GDF15 led to an increased number of cFos$^+$ cells that appear to be additive, but without statistical significance in comparisons with animals dosed with GIPRA or GDF15 alone (Fig. 7*M*). In the BST, GIPRA and GDF15 treatments both led to increased numbers of cFos$^+$ cells compared with the vehicle group, and the combination of these treatments led to similar cFos expression compared with each agent alone (Fig. 7*N*). The PBN is a major neuronal center responsible for the transmission of noxious/aversive signals to areas of the CNS associated with control of both appetite and nausea (34). Interestingly, treatment with PYY induced cFos expression in the PBN, while this effect was moderately reduced in animals receiving cotreatment of PYY and GIPRA (Fig. 7*O*). In summary, when comparing the effect of GIPRA on neuronal activity induced by PYY or GDF15, we found that consistent with its antiaversive action, GIPRA moderately reduced PYY-induced neuronal activity in the PBN.

GIPRA Suppressed PYY-Induced Activity in the Dorsal Subnucleus of PBN

Since the PBN encapsules different neuronal populations with a high degree of heterogeneity (34), we further characterized cFos$^+$ signals in subdomains of the PBN. Surprisingly, LAPYY analog treatment induced strong cFos

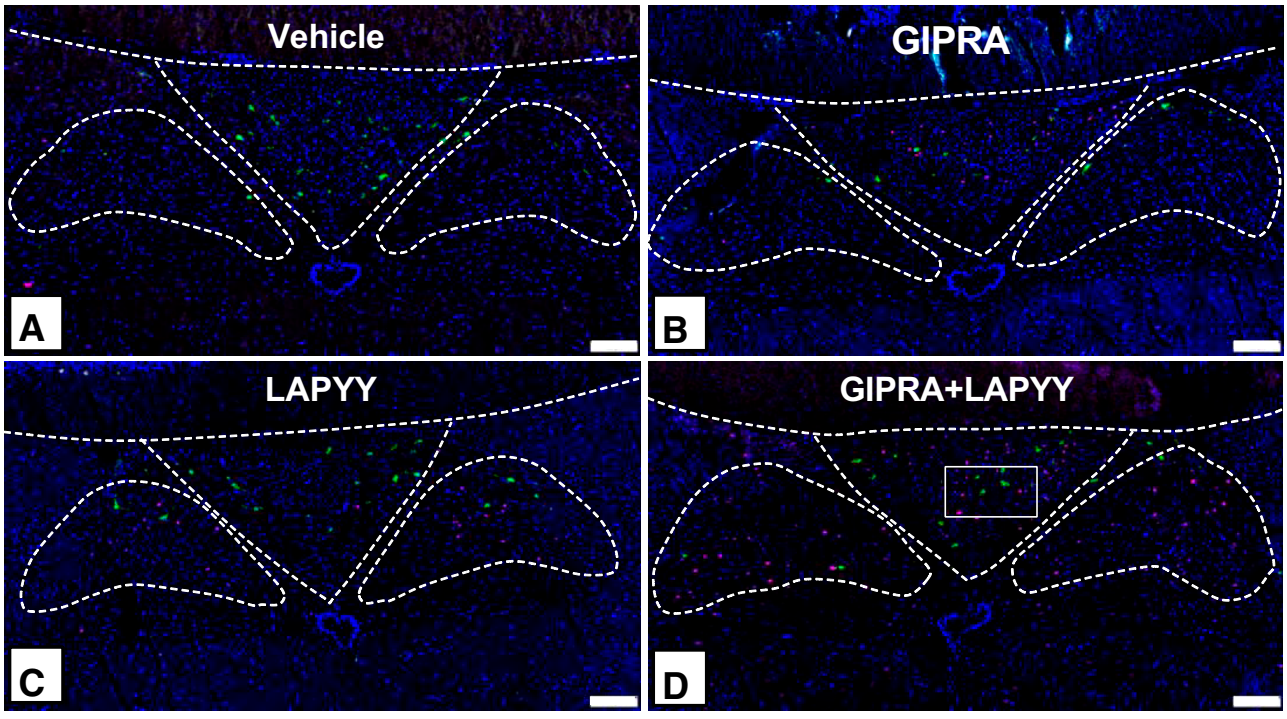

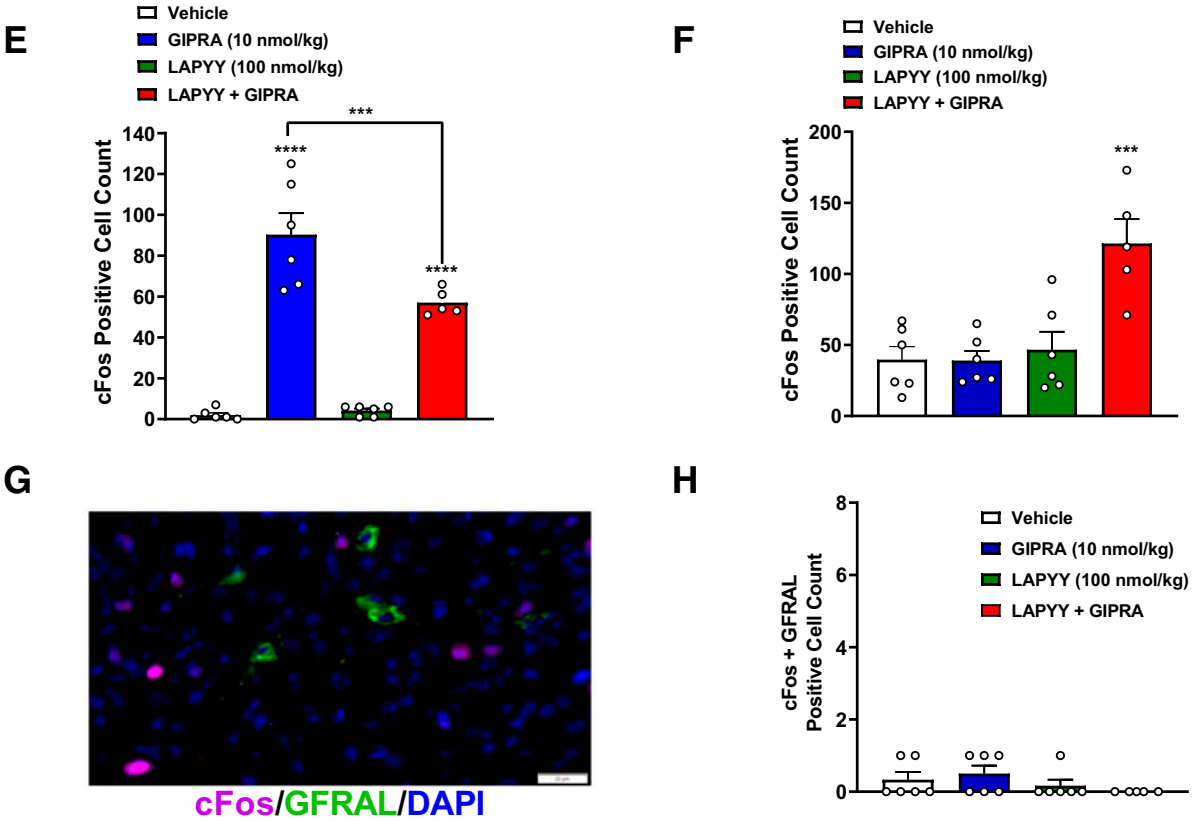

Figure 6—Activation of brainstem neurons by GIPRA and LAPYY at 45 min posttreatment. Representative brainstem immunofluorescent images of mice receiving vehicle (*A*), a GIPRA (10 nmol/kg) (*B*), an LAPYY analog (100 nmol/kg) (*C*), and GIPRA + LAPYY analog (*D*) ($n = 6$ per group). Neuronal activities ($cFos^+$ cell counts) in the AP (*E*) and NTS (*F*) at 45 min postinjection were quantified. *G*: High-magnification image representing the square in *D* shows nonoverlapping pattern of cFos and growth differentiation factor 15 receptor (GFRAL). *H*: Quantification of cFos and GFRAL double-positive cells in AP. For all immunofluorescent images, cFos, purple; GFRAL, green; DAPI, blue. Values are means ± SEM. Statistical analyses included one-way ANOVA followed by Dunnett multiple comparison test. ***$P < 0.001$; ****$P < 0.0001$. Scale bars in *A*–*D*: 100 μm. Scale bar in *G*: 10 μm.

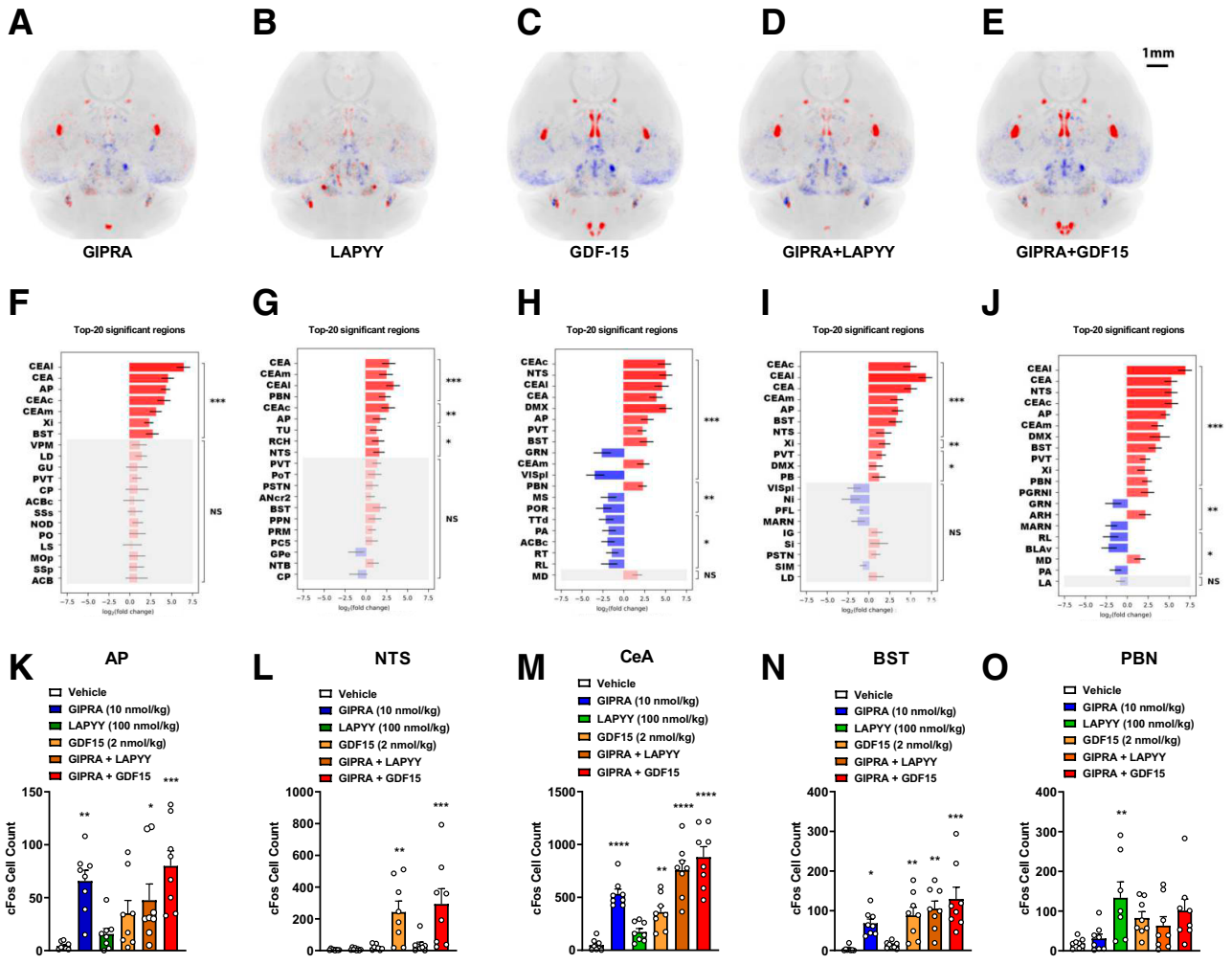

Figure 7—Distinct brain cFos patterns at 120 min after GIPRA, LAPYY analog, and GDF15 treatments. Averaged group overview (dorsal view) of changes in cFos activity relative to the vehicle group (n = 8) (*A–I*). Brain regions where the number of cFos cells is increased in comparison with the vehicle group are shown in red and regions with reduced cFos count compared with vehicle group are shown in blue. Unbiased whole brain analysis of cFos fold induction by GIPRA (*F*), LAPYY analog (*G*), GDF15 (*H*), GIPRA + LAPYY analog (*I*), and GIPRA + GDF15 (*J*) with the top 20 brain regions with statistically significant cFos changes compared with vehicle shown. *K–O*: Quantification of cFos cell counts in different brain regions. Values are means ± SEM. Statistical analyses performed included one-way *ANOVA* followed by Dunnett multiple comparison test. *$P < 0.05$; **$P < 0.005$; ***$P < 0.001$; ****$P < 0.0001$. ACB, nucleus accumbens; ACBc, nucleus accumbens core; ANcr2, Crus II; ARH, arcuate nucleus of hypothalamus; BLAv, basolateral amygdala ventral part; CEAc, central amygdala capsular part; CEAl, central amygdala lateral part; CEAm, central amygdala medial part; CP, caudoputamen; GPe, globus pallidus external part; GRN, gigantocellular reticular nucleus; GU, gustatory areas; IG, indusium griseum; LA, lateral amygdala; LD, lateral dorsal nucleus of thalamus; LS, lateral septum; MARN, magnocellular reticular nucleus; MD, medial dorsal thalamus; MOp, primary motor area; MS, medial septum; NOD, nodulus(X); Ni, nucleus incertus; NS, not significant; NTB, nucleus of the trapezoid body; PA, posterior amygdala; PC5, parvocellular motor 5; PO, posterior complex of the thalamus; PFL, paraflocculus; PGRNl, paragigantocellular reticular nucleus lateral part; POR, postrhinal cortex; PoT, posterior triangular thalamus; PPN, pedunculopontine; PRM, paramedian lobule; PSTN, parasubthalamic nucleus; PVT, paraventricular thalamus; RCH, retrochiasmatic area; RL, rostral linear nucleus raphe; RT, reticular nucleus of the thalamus; Si, substantia innominata; SIM, simple lobule; SSp, primary somatosensory area; SSs, supplemental somatosensory area; TTd, tenia tecta dorsal part; TU, tuberal nucleus; VISpl, posterolateral visual area; VPM, ventral posteromedial nucleus of the thalamus; Xi, xiphoid thalamus.

expression in the PBN_D (green arrow in Fig. 8*B* and *F*) that is spatially separate from the PBN_V activated by GDF15 (yellow arrow in Fig. 8*C* and *F*). In addition, LAPYY analog–induced cFos expression in the PBN_D appeared to be reduced in the GIPRA and PYY cotreatment group (Fig. 8*D*). Quantification of $cFos^+$ cells within the three-dimensional PBN_D and PBN_V (Fig. 8*G*) (see *RESEARCH DESIGN AND METHODS*) confirmed that LAPYY treatment led to significantly increased cFos expression in the PBN_D and a small increase of cFos expression in the PBN_V, while GDF15 treatment resulted in high cFos expression in the PBN_V but not in the PBN_D (Fig. 8*H* and *I*). Importantly, the number of $cFos^+$ cells in the PBN_D was reduced in animals receiving cotreatment of the GIPRA and LAPYY in comparison with the LAPYY analog treatment group (Fig. 8*H*). Interestingly, PBN_D neurons activated by the LAPYY

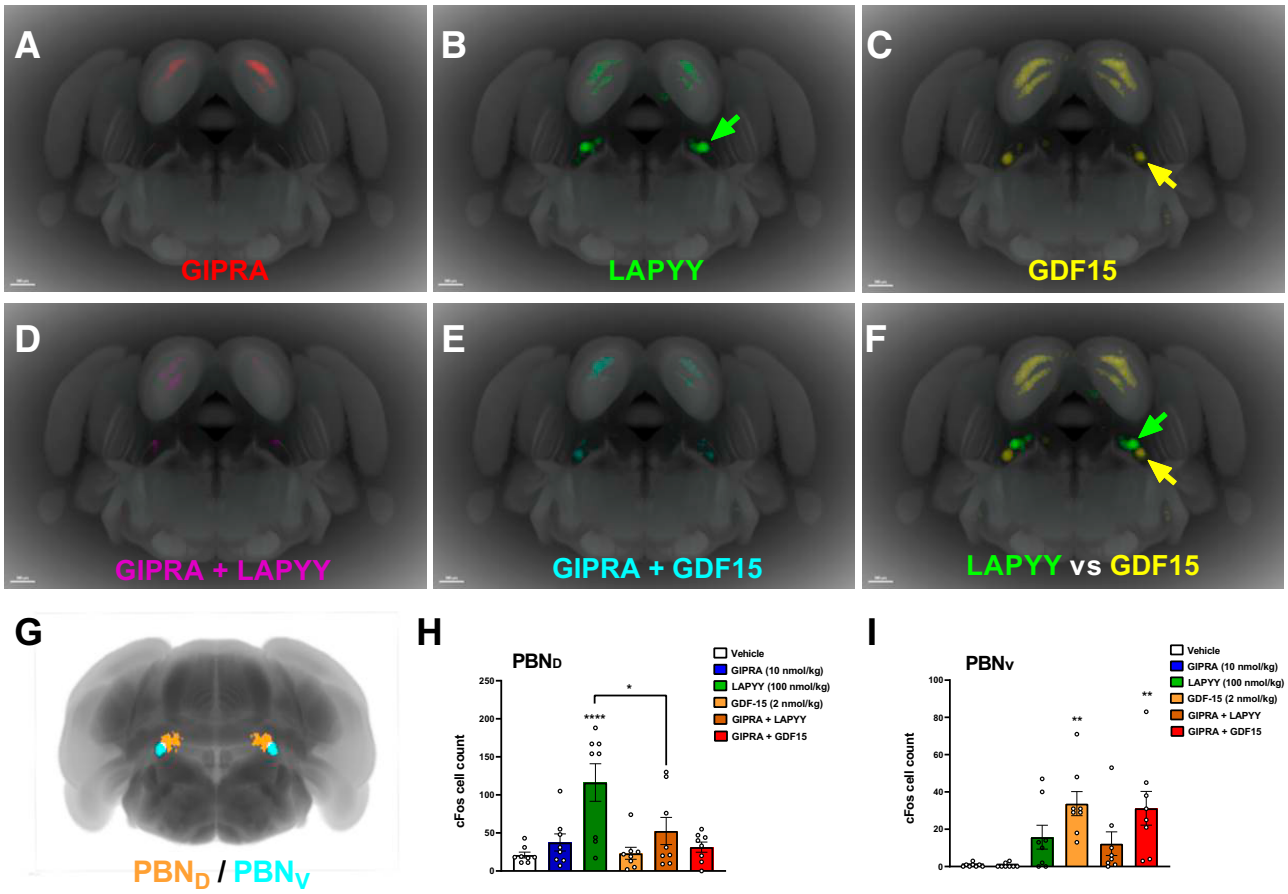

Figure 8— PBN_D is specifically activated by LAPYY analog and inhibited by GIPRA. Averaged group view (n = 8) of cFos activity at coronal section bregma −5 mm from mice dosed subcutaneously with GIPRA alone (*A*), LAPYY analog alone (*B*), GDF15 alone (*C*), GIPRA + LAPYY analog (*D*), and GIPRA + GDF15 (*E*). (F) Virtual overlay of average cFos signal induced by LAPYY in green and by GDF15 in yellow. Note that LAPYY analog and GDF15 activated dorsal-medial (PBN_D) and ventral-lateral (PBN_V) part of the PBN, respectively. *G*: A 100-μm-thick three-dimensional virtual brain slice with PBN_D shown in orange and PBN_V in cyan. (See *RESEARCH DESIGN AND METHODS* for details.) *H*: cFos cell count in three-dimensional PBN_D. *I*: cFos cell count in three-dimensional PBN_V. Scale bars in panel *A–F*: 500 μm. Values in *H* and *I* are means ± SEM. Statistical analyses included one-way ANOVA followed by Dunnet multiple comparisons test. *$P < 0.05$; **$P < 0.005$; ****$P < 0.0001$.

analog do not express CGRP or FoxP2 (arrowheads in Supplementary Fig. 6). In summary, here we show for the first time that an LAPYY analog stimulates cFos expression in a subnucleus of the PBN (PBN_D), distinct from GDF15-stimulated neurons in PBN_V. Furthermore, a GIPRA suppressed LAPYY-induced neuronal activity in PBN_D. These data provide a potential explanation for how GIPR agonism blocks PYY-induced CTA. Future neural circuitry studies are required to fully test this hypothesis.

DISCUSSION

The major findings of the current study are that GIPR agonists inhibit PYY-induced aversion but not PYY-mediated reductions in food intake. Mechanistically, our findings suggest that the antiaversive efficacy of GIPR agonism is underlined by the inhibition of PYY-induced neuronal activity in a subpopulation of neurons located in the PBN, a known relay center for nauseating stimuli.

Analogs of PYY are potential drug candidates for the treatment of obesity and type 2 diabetes (35). However, the appetite-suppressing and emetic actions of PYY are hypothesized to be driven by overlapping neuronal circuits (24). To date, the occurrence of nausea/emesis has undermined the clinical application of PYY-based medicines (27). Consequently, several strategies have been implemented with the aim of bypassing such tolerability issues (27). Indeed, cotreatment with low doses of PYY and glucagon-like peptide 1 are well tolerated and deliver improved appetite suppression in healthy and obese participants (36–38). Further, an engineered long-acting PYY-antibody conjugate to achieve low but sustained NPY2R engagement reduces food intake with minimal emetic action in nonhuman primates (27). A key finding of our studies is that although GIPR agonism was unable to block the aversive response of LiCl or GDF15, both of which induce a state of visceral malaise, peripheral and central GIPR agonism inhibited the aversive effect of an LAPYY analog, without affecting its

anorectic activity (33). These results therefore indicate that it is possible to separate the hypophagic and aversive effects of PYY and that the antiaversive action of GIPR agonism may be specific to satiety factors. Taken together, our data provide evidence supporting the notion that GIP is an effective antiaversive hormone, in response to gastrointestinal-derived satiation signals. Consistent with this notion, the GIPR is expressed by a population of inhibitory (GABAergic) neurons in the AP (12), an area of the brain that plays a key role in the response to emetic stimuli (7). Peripherally administered GIP stimulates neuronal activity and augments the anorectic efficacy of GLP-1R agonism (15). Further, the administration of a GIPRA blocks glucagon-like peptide 1–mediated emesis in the musk shrew (18,39). Thus, since a major challenge to the therapeutic utility of weight loss medications is dose-limiting nausea/vomiting (2,3), our findings have therapeutic relevance in indicating that GIPR agonism could be leveraged to offset tolerability issues that occur with many diabetes medications.

In support of GIP action in the brainstem, the GIPR is expressed by neurons in the AP (12,13). Further, we found that peripheral administration of a GIPRA induced neuronal activity (cFos) in the AP and central administration of the GIPRA suppressed the aversive action of an LAPYY agonist. Moreover, consistent with the differential effect of the GIPRA on PYY- and GDF15–induced CTA, we found that the GIPR and NPY2R are expressed by an overlapping population of neurons in the AP, while it has been reported that the GIPR and GFRAL are expressed by separate populations of neurons in the AP (13). Therefore, to determine whether the GIPRA reduced PYY-induced CTA, but not that of GDF15, due to the engagement of distinct neuronal circuits downstream of receptor activation, we conducted whole-brain cFos analyses. From this approach, we found that both the GIPRA and GDF15 induced neuronal activity in several brain regions linked with the control of appetite and defense against the consumption of toxic stimuli. Importantly, the GIPRA reduced the dorsal PBN activity stimulated by PYY, while the GIPRA had no effect on GDF15-induced neuronal activity in any brain regions.

The PBN is a known relay center for sensory information (visceral malaise, taste, temperature, and pain) and is reported to be critical in the delivery of such information to other brain areas including the hypothalamus, CeA, and BST (34). Importantly, CGRP-expressing neurons located in the PBN have been shown to play an essential role in the acquisition and expression of CTA following exposure to several known aversive agents (8). Interestingly, our whole-brain analysis identified the PBN_D as a novel brain region activated on the administration of an LAPYY analog. The PBN_D is spatially distinct from the CGRP-expressing PBN_V activated by GDF15. Importantly, we found that GIPRA treatment suppressed PYY-stimulated cFos expression in the PBN_D but not GDF15-induced cFos expression in the PBN_V. This finding is consistent with GDF15 and the GIPRA acting on separate neuronal populations in the AP and indicates a potential neuronal mechanism by which the GIPRA suppresses PYY-produced CTA but has no effect on the aversive behavior caused by GDF15. Although GDF15 responsive and CGRP-expressing PBN_V neurons are well characterized (9,34), the roles of PYY-responsive PBN_D neurons we identified here are less well understood. Many distinct subpopulations of neurons exist within dorsal PBN subnuclei and play different biological roles. For example, $FoxP2^+$ neurons in the PBN_D were shown to respond to palatable food, hypotension, sodium depletion, and changes in temperature (40–42). Prodynorphin (Pdyn)-expressing neurons of the PBN, which partially overlap with $FoxP2^+$ cells, have been shown to be activated by digestive tract distension, heat, and noxious pain stimuli (42–44). In addition, Oxtr-expressing PBN neurons play a key role in the regulation of thirst (45). Thus, the PYY-responsive cells we identified in the PBN_D likely represent a novel population of neurons, whose identity and function deserve future study. Nonetheless, our findings that GIPR agonism suppresses PYY-induced neuronal activation in the PBN_D, but not in the CGRP-expressing PBN_V, suggest that GIP may mediate its antiaversive efficacy via a novel neuronal pathway. In summary, here, we describe a novel neural mechanism in the AP and the PBN that appears to underlie the antiaversive action of GIPR agonism. Future studies are necessary to fully determine the neural mechanisms for the anorectic and antiaversive action of GIPR agonism.

Summary

A major barrier to the effectiveness of many current and investigative appetite-suppressing agents is the co-occurrence of nausea and emesis. Here, we used PYY-induced appetite suppression and CTA as a model system to investigate the antiaversive action of GIPR agonism. We demonstrated that treatment with both GIPRA and LAGIPRA attenuates visceral malaise induced by an LAPYY analog, without impacting appetite suppression. Further, we show that peripheral administration of a short-acting GIP induces neuronal activity in the AP and that central administration of GIP blocks PYY-induced aversive behavior in mice. Mechanistically, our study suggests that the ability of GIP to suppress aversive behavior produced by PYY may be underlined by reduced neuronal activity in a subdivision of the PBN, an area of the brain linked with the regulation of aversive behavior. Future studies will determine whether this region of the brain is required for both the appetite-suppressing and antiaversive efficacy of GIPR agonism.

Acknowledgments. The authors thank Mathew P. Coghlan, Julie S. Moyers, Mathijs Bunck, and Paul K. Owens, all from Lilly Research Laboratories, Lilly Corporate Center, Indianapolis, IN, for helpful discussions on the topics of this manuscript. The authors thank Pernille Barkholt, Jacob Hecksher-Sørensen, and Ditte Dencker Thorbek, all from Gubra ApS, Hørsholm, Denmark, for technical support.

Duality of Interest. R.J.S., R.C., B.M.S., E.C.F., B.A.D., D.A.B., J.D., M.D., J.A.-F., T.C., K.W.S., P.J.E., and M.A. are current or past employees of Eli Lilly and Company. B.C.D.J. and M.R.H. receive research funding for an investigator-initiated proposal from Eli Lilly and Company. No other potential conflicts of interest relevant to this article were reported.

Author Contributions. R.C., E.C.F., and B.A.D. performed CTA and glucose tolerance assays. B.M.S. conducted mouse cFos studies. M.D. conducted PK analysis. J.D. performed in vitro assays. D.A.B., J.A.-F., T.B., B.C.D.J., M.R.H., T.C., and K.W.S. contributed to data interpretation and writing of the manuscript. R.J.S., P.J.E., and M.A. were responsible for study conception, experimental designs, data analyses and interpretation, and drafting and editing of the manuscript. R.J.S. is the guarantor of this work and, as such, had full access to all the data in the study and takes responsibility for the integrity of the data and the accuracy of the data analysis.

References

1. Bettge K, Kahle M, Abd El Aziz MS, Meier JJ, Nauck MA. Occurrence of nausea, vomiting and diarrhoea reported as adverse events in clinical trials studying glucagon-like peptide-1 receptor agonists: a systematic analysis of published clinical trials. Diabetes Obes Metab 2017;19:336–347

2. Williams DM, Nawaz A, Evans M. Drug therapy in obesity: a review of current and emerging treatments. Diabetes Ther 2020;11:1199–1216

3. Srivastava G, Apovian CM. Current pharmacotherapy for obesity. Nat Rev Endocrinol 2018;14:12–24

4. Saper CB. The house alarm. Cell Metab 2016;23:754–755

5. Horn CC. Why is the neurobiology of nausea and vomiting so important? Appetite 2008;50:430–434

6. Andermann ML, Lowell BB. Toward a wiring diagram understanding of appetite control. Neuron 2017;95:757–778

7. Miller AD, Leslie RA. The area postrema and vomiting. Front Neuroendocrinol 1994;15:301–320

8. Chen JY, Campos CA, Jarvie BC, Palmiter RD. Parabrachial CGRP neurons establish and sustain aversive taste memories. Neuron 2018;100:891–899.e5

9. Carter ME, Han S, Palmiter RD. Parabrachial calcitonin gene-related peptide neurons mediate conditioned taste aversion. J Neurosci 2015;35:4582–4586

10. Campbell JE, Drucker DJ. Pharmacology, physiology, and mechanisms of incretin hormone action. Cell Metab 2013;17:819–837

11. Adriaenssens AE, Gribble FM, Reimann F. The glucose-dependent insulinotropic polypeptide signaling axis in the central nervous system. Peptides 2020;125:170194

12. Adriaenssens AE, Biggs EK, Darwish T, et al. Glucose-dependent insulinotropic polypeptide receptor-expressing cells in the hypothalamus regulate food intake. Cell Metab 2019;30:987–996.e6

13. Zhang C, Kaye JA, Cai Z, Wang Y, Prescott SL, Liberles SD. Area postrema cell types that mediate nausea-associated behaviors. Neuron 2021;109:461–472.e5

14. Costa A, Ai M, Nunn N, et al. Anorectic and aversive effects of GLP-1 receptor agonism are mediated by brainstem cholecystokinin neurons, and modulated by GIP receptor activation. Mol Metab 2022;55:101407

15. Zhang Q, Delessa CT, Augustin R, et al. The glucose-dependent insulinotropic polypeptide (GIP) regulates body weight and food intake via CNS-GIPR signaling. Cell Metab 2021;33:833–844.e5

16. Mroz PA, Finan B, Gelfanov V, et al. Optimized GIP analogs promote body weight lowering in mice through GIPR agonism not antagonism. Mol Metab 2019;20:51–62

17. Finan B, Ma T, Ottaway N, et al. Unimolecular dual incretins maximize metabolic benefits in rodents, monkeys, and humans. Sci Transl Med 2013;5:209ra151

18. Borner T, Geisler CE, Fortin SM, et al. GIP receptor agonism attenuates GLP-1 receptor agonist–induced nausea and emesis in preclinical models. Diabetes 2021;70:2545–2553

19. Taiji A, Nishizawa N, Niida A, et al. GIP receptor activating peptide (patent WO2018181864). World Intellectual Property Organization International Bureau. Accessed 4 October 2018. Available from https://patentimages.storage.googleapis.com/97/6a/db/f82f923d4d828f/WO2018181864A1.pdf

20. Samms RJ, Coghlan MP, Sloop KW. How may GIP enhance the therapeutic efficacy of GLP-1? Trends Endocrinol Metab 2020;31:410–421

21. Hayes MR, Borner T, De Jonghe BC. The role of GIP in the regulation of GLP-1 satiety and nausea. Diabetes 2021;70:1956–1961

22. Samms RJ, Sloop KW, Gribble FM, Reimann F, Adriaenssens AE. GIPR function in the central nervous system: implications and novel perspectives for GIP-basedz therapies in treating metabolic disorders. Diabetes 2021;70:1938–1944

23. le Roux CW, Borg CM, Murphy KG, Vincent RP, Ghatei MA, Bloom SR. Supraphysiological doses of intravenous PYY3-36 cause nausea, but no additional reduction in food intake. Ann Clin Biochem 2008;45:93–95

24. Halatchev IG, Cone RD. Peripheral administration of PYY(3-36) produces conditioned taste aversion in mice. Cell Metab 2005;1:159–168

25. Batterham RL, Cowley MA, Small CJ, et al. Gut hormone PYY(3-36) physiologically inhibits food intake. Nature 2002;418:650–654

26. De Silva A, Bloom SR. Gut hormones and appetite control: a focus on PYY and GLP-1 as therapeutic targets in obesity. Gut Liver 2012;6:10–20

27. Rangwala SM, D'Aquino K, Zhang YM, et al. A long-acting PYY_{3-36} analog mediates robust anorectic efficacy with minimal emesis in nonhuman primates. Cell Metab 2019;29:837–843.e5

28. Østergaard S, Jessen C, Wulff BS, Sanfridson A. Selective pyy compounds and uses thereof (patent WO2016198682). World Intellectual Property Organization International Bureau. Accessed 15 December 2016. Available from https://patentimages.storage.googleapis.com/96/39/a8/2f42ef61c8b749/WO2016198682A1.pdf

29. Coskun T, Sloop KW, Loghin C, et al. LY3298176, a novel dual GIP and GLP-1 receptor agonist for the treatment of type 2 diabetes mellitus: from discovery to clinical proof of concept. Mol Metab 2018;18:3–14

30. Briere DA, Bueno AB, Gunn EJ, Michael MD, Sloop KW. Mechanisms to elevate endogenous GLP-1 beyond injectable GLP-1 analogs and metabolic surgery. Diabetes 2018;67:309–320

31. Worth AA, Shoop R, Tye K, et al. The cytokine GDF15 signals through a population of brainstem cholecystokinin neurons to mediate anorectic signalling. eLife 2020;9:e55164

32. Perens J, Salinas CG, Skytte JL, et al. An optimized mouse brain atlas for automated mapping and quantification of neuronal activity using iDISCO+ and light sheet fluorescence microscopy. Neuroinformatics 2021;19:433–446

33. Borner T, Shaulson ED, Ghidewon MY, et al. GDF15 induces anorexia through nausea and emesis. Cell Metab 2020;31:351–362.e5

34. Palmiter RD. The parabrachial nucleus: CGRP neurons function as a general alarm. Trends Neurosci 2018;41:280–293

35. Gimeno RE, Briere DA, Seeley RJ. Leveraging the gut to treat metabolic disease. Cell Metab 2020;31:679–698

36. Schmidt JB, Gregersen NT, Pedersen SD, et al. Effects of PYY3-36 and GLP-1 on energy intake, energy expenditure, and appetite in overweight men. Am J Physiol Endocrinol Metab 2014;306:E1248–E1256

37. Neary NM, Small CJ, Druce MR, et al. Peptide YY3-36 and glucagon-like peptide-17-36 inhibit food intake additively. Endocrinology 2005;146:5120–5127

38. De Silva A, Salem V, Long CJ, et al. The gut hormones PYY 3-36 and GLP-1 7-36 amide reduce food intake and modulate brain activity in appetite centers in humans. Cell Metab 2011;14:700–706

39. Geisler C, Borner T, Gaisinsky J, et al. GIP receptor agonism attenuates GLP-1 receptor agonist induced nausea in rodents. Obesity (Silver Spring) 2020;28:103

40. Rodriguez E, Ryu D, Zhao S, Han BX, Wang F. Identifying parabrachial neurons selectively regulating satiety for highly palatable food in mice. eNeuro 2019;6:ENEURO.0252-19.2019
41. Stein MK, Loewy AD. Area postrema projects to FoxP2 neurons of the pre-locus coeruleus and parabrachial nuclei: brainstem sites implicated in sodium appetite regulation. Brain Res 2010;1359:116–127
42. Geerling JC, Kim M, Mahoney CE, et al. Genetic identity of thermosensory relay neurons in the lateral parabrachial nucleus. Am J Physiol Regul Integr Comp Physiol 2016;310:R41–R54
43. Kim DY, Heo G, Kim M, et al. A neural circuit mechanism for mechanosensory feedback control of ingestion. Nature 2020;580:376–380
44. Chiang MC, Nguyen EK, Canto-Bustos M, Papale AE, Oswald AM, Ross SE. Divergent neural pathways emanating from the lateral parabrachial nucleus mediate distinct components of the pain response. Neuron 2020;106: 927–939.e5
45. Ryan PJ, Ross SI, Campos CA, Derkach VA, Palmiter RD. Oxytocin-receptor-expressing neurons in the parabrachial nucleus regulate fluid intake. Nat Neurosci 2017;20:1722–1733